

Characteristics of Al₂O₃-Pt/YSZ-Pt Double Layer Composite Coatings Prepared by Cathode Plasma Electrolytic Deposition

Deng Shunjie¹, Jiang Chi², Liu Tianwei², Shuai Maobing¹, Wang Peng³

¹ Science and Technology on Surface Physics and Chemistry Laboratory, Mianyang 621907, China; ² China Academy of Engineering Physics, Mianyang 621900, China; ³ Research Institute of Aerospace Special Materials and Processing Technology, Beijing 100076, China

Abstract: Al₂O₃-Pt/YSZ-Pt double layer composite coatings were prepared by cathode plasma electrolytic deposition (CPED) on the superalloy with a NiCoCrAlY bond-coat. The composite coatings consist of an Al₂O₃-Pt film and a YSZ-Pt top-coat and show a good adhesion to the metallic bond-coat. It is demonstrated, from the cyclic oxidation test and mechanical properties test, that such coatings possess good oxidation and spallation resistance. These beneficial results can be attributed to these effects: owing to the extremely low oxygen diffusion rate of Al₂O₃-Pt film, such composite coatings can inhibit further oxidation of the bond-coat; the mechanical properties of Al₂O₃-Pt/YSZ-Pt composite coating are improved by the toughening effect of Pt particles.

Key words: cathode plasma electrolytic deposition; high-temperature oxidation resistance; composite coating; toughening effect

With the demand of high thrust-to-weight ratio and fuel efficiency of the engines, the gas inlet temperature of the engine is strongly demanded to be improved^[1]. Consequently, thermal barrier coatings (TBCs) with low-thermal conductivity have been widely used to protect metallic components from the hot gas stream^[2, 3]. Currently, typical TBCs are usually composed of a heat insulating top-coat of Y₂O₃-stabilized ZrO₂ (YSZ), a metallic bond-coat and a superalloy substrate. The metallic bond-coat can provide good adhesion and strong oxidation protection for the superalloy substrate^[4]. However, at elevated temperatures, the permeation of oxygen through the YSZ top-coat results in the formation of a thermally grown oxide (TGO) layer at the bond-coat/top-coat interface. An ideal TGO layer mainly consists of α -Al₂O₃ and can prevent further oxidation of the bond-coat. However, it has been certified that the failure of TBC systems usually takes place at the top-coat from the TGO layer or at TGO/bond-coat interface^[5-7]. First, other spinel-type oxides such as (Cr,Al)₂O₃, Ni(Cr,Al)₂O₄ and NiO with a rapid local volume increase and a high oxygen diffusion rate^[8-10]

sometimes form in the TGO layer. Second, the thermal expansion mismatch between the TGO layer and the bond-coat results in high thermal stresses in the TGO layer^[11,12]. Once the thermal stresses increase and exceed the critical crack propagation stress of the TGO layer, the crack propagation occurs in the TGO layer^[13,14]. Therefore, the key to enhancing the service life of current TBCs is to improve the oxidation resistance of the metallic bond-coat, reduce the stress growth rate of the TGO layer and release the stress in TGO layer^[15,16].

In recent decades, extensive attentions have been focused on the improvement of the metallic bond-coat oxidation resistance by either applying over-aluminizing treatments^[17-20], or performing pre-oxidation of the bond-coat^[21] or high-current pulsed electron beam irradiating coating surfaces^[9]. Recently, a novel approach is proposed to enhance the high-temperature oxidation resistance of the metallic bond-coat. A thin Al₂O₃ film is prepared on the bond-coat before the deposition of ceramic top-coat to improve the oxidation resistance of the bond-coat^[22]. However, owing to

Received date: January 22, 2018

Foundation item: National Natural Science Foundation of China (51271030, 51801191); China Postdoctoral Science Foundation (2017M623066)

Corresponding author: Shuai Maobing, Ph. D., Professor, Science and Technology on Surface Physics and Chemistry Laboratory, Mianyang 621907, P. R. China, Tel: 0086-816-3620185, E-mail: shuaimb@sina.com

Copyright © 2018, Northwest Institute for Nonferrous Metal Research. Published by Elsevier BV. All rights reserved.

the poor mechanical properties of the Al_2O_3 film, Al_2O_3 film is easily peeled off from the bond-coat at a high temperature. It is reported that the high-temperature spallation resistance of the ceramic coating can be improved by doping noble metallic particles, which possess outstanding high-temperature stability and mechanical properties^[23]. Different ceramic coatings doped with noble nano-particles, possessing good high-temperature spallation resistance, have been fabricated, such as $\text{Al}_2\text{O}_3\text{-Au}$ ^[24], $\text{La}_2\text{Zr}_2\text{O}_7\text{-Pt}$ ^[25] and $\text{Al}_2\text{O}_3\text{-Pt/YSZ-Pt}$ composite coatings^[7]. Hence, it should be an effective way for improving the mechanical properties of the thin Al_2O_3 film by doping dispersed noble metallic particles. Consequently, the oxidation resistance of the metallic bond-coat and the service life of TBC system can be improved.

In this work, cathode plasma electrolytic deposition (CPED) was applied to prepare these composite coatings. Such method is a combination of conventional electrolysis and plasma process, which has been studied for decades^[26-30]. A thin Al_2O_3 coating doped with Pt particles was prepared firstly on the metallic bond-coat, and then a YSZ top-coat doped with Pt particles was deposited on this thin $\text{Al}_2\text{O}_3\text{-Pt}$ coating. The high-temperature oxidation resistance and mechanical properties of such composite coatings were investigated, and the mechanisms of such effect have been discussed.

1 Experiment

1.1 Coating preparation

The schematic view of CPED device for preparing $\text{Al}_2\text{O}_3\text{-Pt/YSZ-Pt}$ composite coatings is shown in Fig.1. A platinum electrode with a dimension of 120 mm×50 mm×0.3 mm was used as the anode. The samples of IC10 alloys (wt%) (0.1 C, 12 Co, 6.5 Cr, 6.2 Al, 5 W, 1 Mo, 1.5 Hf, 6.5 Ta, 0.01 B, balance Ni) were used as the cathode with a size of 15 mm×10 mm×2 mm. Then Praxair 3710 type APS equipment was used for the preparation of NiCoCrAlY with a thickness of 120 μm on the IC10 alloys. And the chemical composition of the NiCoCrAlY bond-coat is Ni-32Co-21Cr-8Al-0.5Y (wt%). A pulsed electrical power supply (TN-KGZ01) was connected to the electrolytic bath. The $\text{Al}_2\text{O}_3\text{-Pt}$ intermediate films were firstly prepared on the coatings 2, 3 and 4. The electrolyte composition and CPED parameters for the preparation of $\text{Al}_2\text{O}_3\text{-Pt}$ films are listed in Table 1. The YSZ-Pt coatings were then prepared on the coatings 1, 2, 3 and 4 and named as samples a, b, c and d, respectively. The electrolyte composition and CPED parameters for preparing YSZ-Pt coatings are listed in Table 2.

1.2 Coating characterization

The morphology of $\text{Al}_2\text{O}_3\text{-Pt/YSZ-Pt}$ coatings was investigated by scanning electron microscope (SEM, JMS-6480A) with an energy-dispersive spectroscopy (EDS) system. The phase structure was detected by X-ray diffraction analysis (XRD, PW 3710, Philips) at room temperature using nickel filtered $\text{Cu K}\alpha$ radiation in a 2θ range of $20^\circ\text{-}90^\circ$ with a step size of 0.02° .

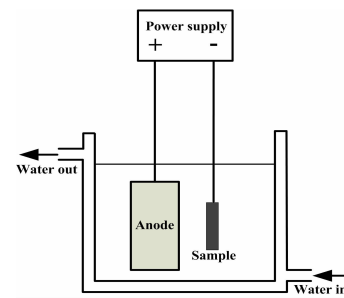


Fig.1 Schematic view of the CPED device

Table 1 Composition of the solution and CPED parameters for preparing $\text{Al}_2\text{O}_3\text{-Pt}$ films on coatings 1~4

Coating	$\text{Al}(\text{NO}_3)_3/\text{mol}\cdot\text{L}^{-1}$	$\text{H}_2\text{PtCl}_6/\text{g}\cdot\text{L}^{-1}$	Voltage/V	Time/min
1	-	-	-	-
2	0.8	0	115	10
3	0.8	0.1	115	10
4	0.8	0.2	115	10

Table 2 Composition of the solution and CPED parameters for preparing $\text{Y}_2\text{O}_3\text{-Pt}$ coatings on samples a~d

Sample	Coating	$\text{Y}(\text{NO}_3)_3/\text{mol}\cdot\text{L}^{-1}$	$\text{Zr}(\text{NO}_3)_4/\text{mol}\cdot\text{L}^{-1}$	$\text{H}_2\text{PtCl}_6/\text{g}\cdot\text{L}^{-1}$	Voltage/V	Time/min
a	1			0	140	30
b	2		0.2	0	140	30
c	3		1.8	0.1	140	30
d	4			0.2	140	30

High temperature cyclic oxidation tests were carried out to investigate the high-temperature oxidation and spallation resistance of the composite coatings in a furnace at 1100°C for 200 h. Before the oxidation test, the mass of sample + crucible (W_0) and crucible (W'_0) were weighed separately by an analytical balance (BT 25S, Sartorius). The sample + crucible were then put into the furnace and taken out after 10 h. After air cooling to room temperature, the spalling oxide could be found in the crucible, and the mass of sample + spalling oxide + crucible (W_1) and spalling oxide + crucible (W'_1) were weighed separately by the analytical balance again. The weight gain is equal to $W_1 - W_0$, and the spallation is equal to $W'_1 - W'_0$. This cycle was then repeated 20 times, the data were recorded and used to evaluate the high-temperature oxidation and spallation resistance of the composite coatings.

Hardness and elastic modulus of the composite coatings were tested by MTS NanoIndenter XP indentation test through driving a diamond indenter into the coating surface, and the depth was kept at 2000 nm. The Vickers indentation testing (Wolpert Wilson Instruments, 401MVD) was used to measure the indentation parameters of half crack length (c), as shown in Fig.2.

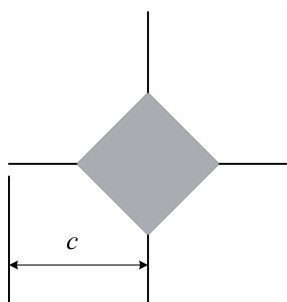


Fig.2 Schematic of Vickers indentation test for measuring half crack length c

2 Results and Discussion

2.1 Morphologies of the prepared coatings

Fig.3 shows the surface morphologies of Al_2O_3 -Pt/YSZ-Pt composite coatings (samples a, b, c and d) prepared by CPED. As shown in Fig.3a and 3b, the surfaces of the sample a and b are rough, and a few cracks can be found in the coatings. The cracks can provide a diffusion path for oxygen, probably resulting in the oxidation of the bond-coat during high temperature service. On the contrary, as shown in Fig. 3c and 3d, no obvious cracks could be observed in the coatings dispersed with Pt particles, which could be beneficial in improving the oxidation resistance of the composite coatings. Moreover, as shown in Fig.3a~3d, several molten areas could be observed on the surface of coatings, owing to the ultra-high temperature locally formed in the plasma discharges during the CPED process.

Fig.4 shows the cross-sectional morphologies of samples a~d prepared by CPED. It can be seen from Fig. 4a that there is no Al_2O_3 film between the YSZ top-coat and the metallic

bond-coat, and the thickness of the YSZ coating is approximately 130 μm . In addition, as shown in Fig.4b~4d, the Al_2O_3 films with a thickness of about 15~20 μm are prepared between the YSZ top-coat and the metallic bond-coat. As the concentration of $\text{H}_2\text{PtCl}_6 \cdot 6\text{H}_2\text{O}$ in solutions increases, the thickness of YSZ coating is increased. Under the same experimental conditions, the thickness of the ceramic coating prepared by CPED is related to the electric conductivity of the coating. During the CPED process, the ceramic coating can be considered as an insulator. Once the ceramic coating is too thick to be broken down, the process of CPED will end. Because of the Pt particles dispersed in the ceramic coating, the conductivity of the coating is improved and then the thickness of the coating can be increased.

Fig.5 shows the SEM-backscattered-electron image of the YSZ coating prepared by CPED on sample d. It can be seen that a lot of Pt particles (white spots), which is proved by EDS analysis, are dispersed in the coating. Fig.6 shows the XRD patterns of the metallic bond-coat, the Al_2O_3 film, the YSZ coating and the YSZ coating after cyclic oxidation. It can be seen that the prepared Al_2O_3 film consists of α - Al_2O_3 and γ - Al_2O_3 , and the prepared YSZ coating consists of $t\text{-Zr}_{0.94}\text{Y}_{0.12}\text{O}_{2.06}$. Additionally, after 200 h of cyclic oxidation, $m\text{-ZrO}_2$ diffraction peaks are clearly detected in the YSZ coating. It is suggested that the phase transformation occurs during the cyclic oxidation.

2.2 High temperature cyclic oxidation properties

Fig.7 shows the oxidation kinetics curves and spallation kinetics curves of samples that were cyclically exposed in an air furnace at 1100 $^\circ\text{C}$ for 200 h. It can be clearly revealed that, compared to the sample with only metallic bond-coat, the samples with Al_2O_3 /YSZ composite coatings possess relatively low oxidation mass gain and spallation mass. In

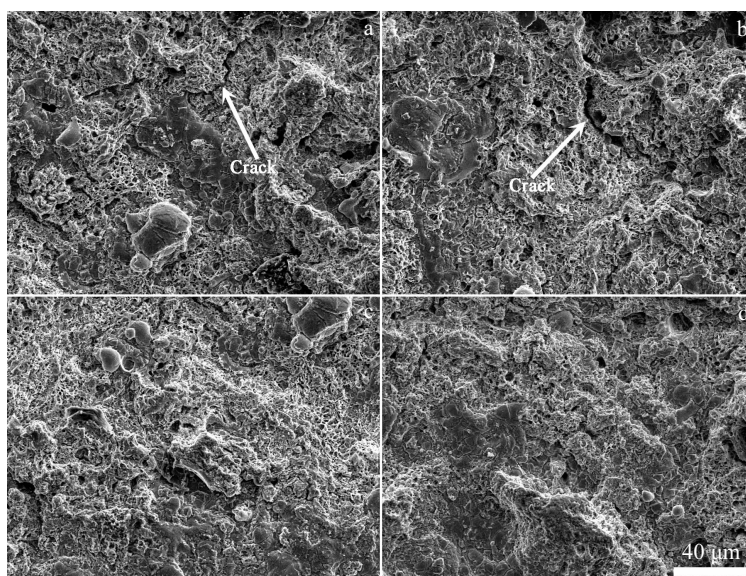


Fig.3 SEM morphologies of coatings prepared on different samples: (a) sample a, (b) sample b, (c) sample c, and (d) sample d

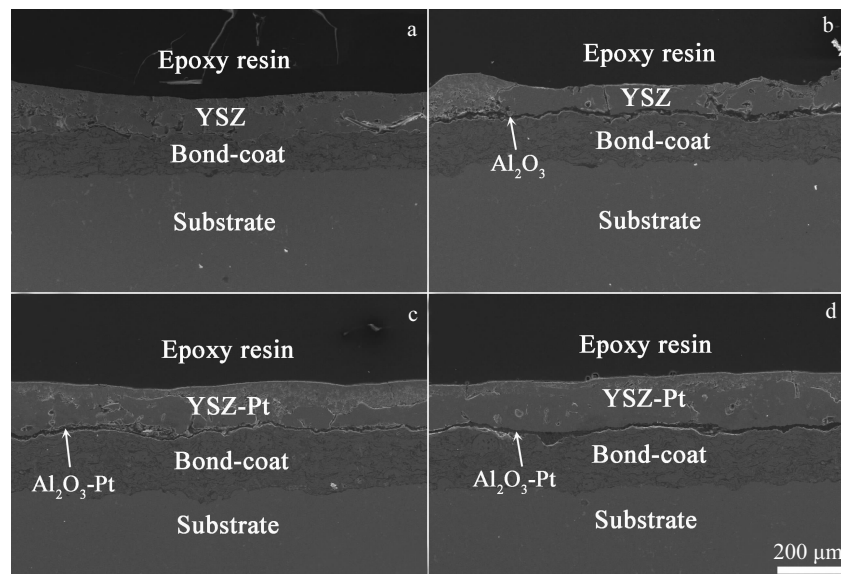


Fig.4 SEM cross-sectional images of coatings prepared on different samples: (a) sample a, (b) sample b, (c) sample c, and (d) sample d

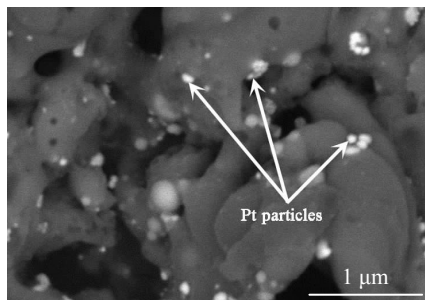


Fig.5 SEM-backscattered-electron image of sample d

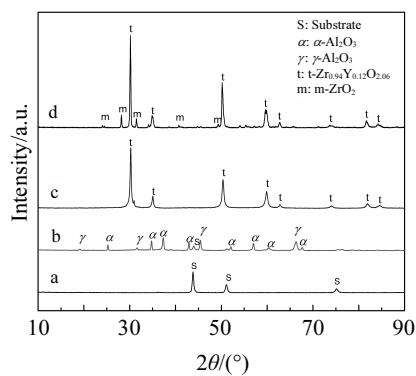


Fig.6 XRD patterns of samples (a-metallic bond-coat, b-Al₂O₃ film, c-YSZ coating, d-YSZ coating after 200 h cyclic oxidation)

addition, the oxidation and spallation resistance can be improved significantly by co-depositing Pt particles, due to the toughening effects of Pt particles dispersed in the Al₂O₃/YSZ composite coatings. For sample a, severe peeling occurred at the metallic bond-coat/YSZ coating interface, since the spallation

mass was sharply increased after 100 h of cyclic oxidation, which can be attributed to the crack initiation and spallation of TGO layer due to the high oxygen diffusion rate of YSZ top-coat. For sample b, in the same way, peeling occurred after 130 h of cyclic oxidation. In contrast, for samples c and d, it can be seen that a larger content of Pt particles results in a better oxidation resistance of the Al₂O₃-Pt/YSZ-Pt composite coatings.

Fig.8 shows the surface morphologies of samples a~d prepared by CPED after cyclic oxidation at 1100 °C. It can be

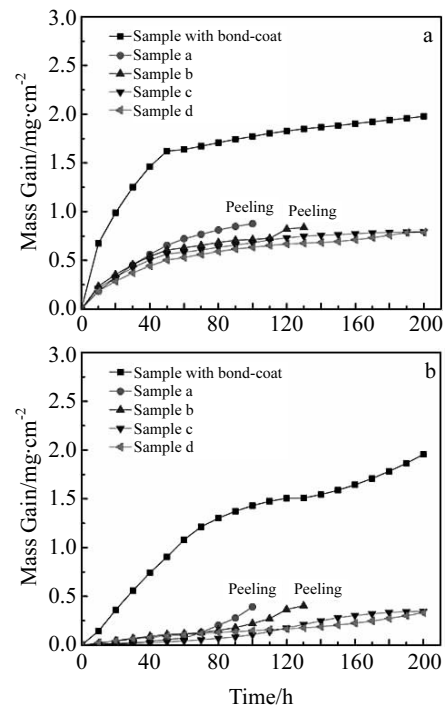


Fig.7 Oxidation kinetic curves (a) and spallation kinetics curves (b) of samples a~d

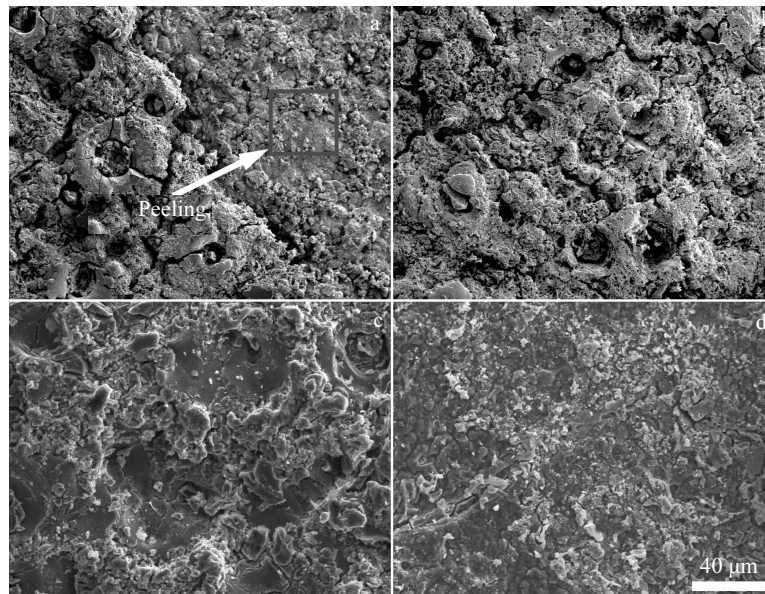


Fig. 8 SEM surface images of coatings after cyclic oxidation tests: (a) sample a, (b) sample b, (c) sample c, and (d) sample d

seen from Fig.8a that lots of cracks are evident on the surface of the coating. In addition, severe peeling of the coating is observed in the red box which is in good agreement with the high-temperature oxidation test result. Fig.9 shows the EDS spectrum of the zone marked in the red box in Fig.8a. It can be found that the selective oxidation of Al in the bond-coat occurs, owing to the high oxygen partial pressure. Furthermore, as the activity and the content of Al for oxidation in the metallic bond-coat decrease, Cr and Co elements will be also oxidized, resulting in the enrichment in Cr and Co on the metallic bond-coat surface. Compared to the sample a shown in Fig.8a, only slight peeling of the coating and a few micro-cracks are observed in Fig. 8b, and according to the EDS results, Al, Cr and Co elements can hardly be detected at the coating surface. Such results can be concluded that the inner Al_2O_3 film with good oxidation resistance can restrict the oxidation of the metallic bond-coat. Furthermore, as shown in Fig.8c and 8d, after 200 h of high-temperature

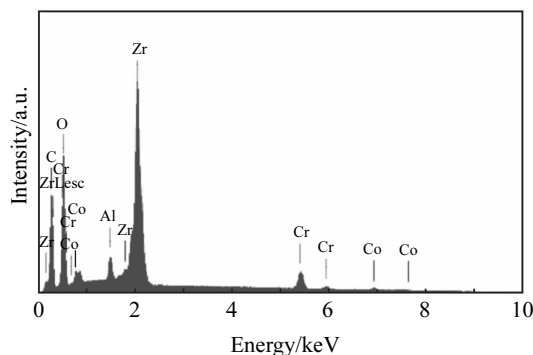


Fig.9 EDS spectrum of zone marked in the red box in Fig.8a

cyclic oxidation, the composite coatings dispersed with Pt particles are intact, and no obvious spallation can be observed on the surfaces of these coatings.

Fig.10 shows the cross-sectional morphologies of samples a~d prepared by CPED after cyclic oxidation at 1100 °C. A part of the coatings without dispersed Pt particles (as shown in Fig.10a and 10b) is peeled off. Comparatively, the Al_2O_3 -Pt/YSZ-Pt composite coatings still maintain an intact and uniform microstructure, and only some micro-cracks without through cracks and buckling can be observed.

2.3 Mechanical properties

Fig.11 shows the elastic modulus and hardness measured on the surfaces of samples a, b, c and d. It can be found that the elastic modulus and hardness of the coating increase as the concentration of $\text{H}_2\text{PtCl}_6 \cdot 6\text{H}_2\text{O}$ in solution increases.

Besides, the Vickers indentation testing was used to measure the indentation parameters of the half crack length c . The crack length was measured immediately after releasing the load, and the fracture toughness was calculated by the following equation^[31]:

$$K_{IC} = 0.016(E/H)^{1/2}(P/c^{3/2}) \quad (1)$$

where K_{IC} is fracture toughness, $\text{MPa}\cdot\text{m}^{1/2}$; P is indenter load (9.8 N); E is elastic modulus, GPa; H is the hardness, GPa; and c is half crack length.

The average fracture toughness of the samples can be calculated by combining Eq.(1) and Fig.11, and the result of the average fracture toughness is shown in Table 3. It can be concluded that the average fracture toughness of the composite coatings is improved as the concentration of $\text{H}_2\text{PtCl}_6 \cdot 6\text{H}_2\text{O}$ in electrolyte increases.

As we know, the thermal expansion coefficient of the oxide coating is much lower than that of the metallic bond-coat.

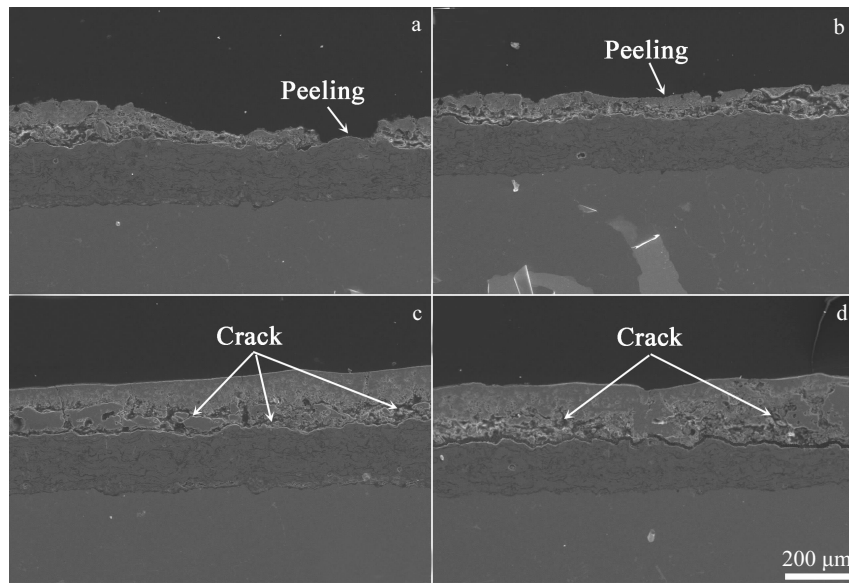


Fig.10 SEM cross-sectional images of coatings after cyclic oxidation tests: (a) sample a, (b) sample b, (c) sample c, and (d) sample d

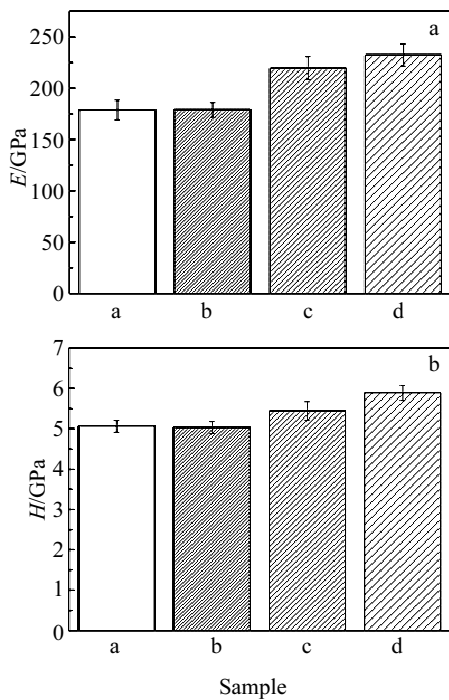


Fig.11 Elastic modulus (a) and the hardness (b) of different samples

During heating-cooling cycles, the oxide coating is subjected to high stresses. In this work, we proposed a method to avoid cracking and peeling of oxide coatings by dispersing Pt particles. From the viewpoint of increasing the mechanical properties of oxide coatings by toughening effects of Pt particles, a brief analysis is discussed as follows. First, during crack propagation, a portion of the fracture energy is absorbed because of the plastic deformation of the Pt particles. Second, the crack tip is blunted during crack propagation because of

Table 3 Mechanical properties of samples a-d

Sample	Average fracture toughness, $K_{IC}/\text{MPa}\cdot\text{m}^{1/2}$	Average elastic modulus E/GPa	Average hardness, H/GPa
a	1.58	178.83	5.08
b	1.62	179.10	5.06
b	1.89	219.71	5.47
d	2.01	232.61	5.92

the relatively large radius of the Pt particles' curvature.

As analyzed by Evans, the spallation of a ceramic coating will take place when the elastic strain energy stored in the coating exceeds the fracture resistance, G_c , of the interface. The criterion for failure is given as the following equation [32]:

$$\frac{(1-\nu)\sigma_{\text{coating}}^2 h}{E_{\text{coating}}} > G_c \tag{2}$$

where h is coating thickness, σ_{coating} is stress in the ceramic coating, ν is Poisson's ratio and E_{coating} is elastic modulus. As discussed above, the thermal stresses can be decreased by dispersing the Pt particles in the coatings, and according to the results shown in Fig.11, the elastic modulus increases as the Pt contents in the composite coating increases. Therefore, the elastic strain energy decreases and the fracture toughness increases, and a better spallation resistance of oxide coating is achieved.

3 Conclusions

1) $\text{Al}_2\text{O}_3\text{-Pt/YSZ-Pt}$ double layer composite coatings prepared by CPED can inhibit further oxidation of the metallic bond-coat owing to the extremely low oxygen diffusion rate of

the Al₂O₃ film.

2) The mechanical properties of Al₂O₃-Pt/YSZ-Pt composite coatings are improved by the toughening effects of Pt particles.

3) The elastic modulus, E_{coating} , of Al₂O₃-Pt/YSZ-Pt composite coating increases with the increase of the Pt contents in coatings.

References

- Mei X X, Liu X F, Wang C X et al. *Apply Surface Science*[J], 2012, 263: 810
- Miller R A. *Journal of Thermal Spray Technology*[J], 1997, 6: 35
- Chen S H, Xiang J Y, Huang J H et al. *Apply Surface Science*[J], 2015, 340: 173
- Padture N P, Gell M, Jordan E H. *Science*[J], 2002, 296: 280
- Evans A G, Hutchinson J W, Meier G H et al. *Progress in Materials Science*[J], 2001, 46: 505
- Lv Brown, Xie H, Xu R et al. *Apply Surface Science*[J], 2016, 360: 461
- Wang P, Deng S J, He Y D et al. *Corrosion Science*[J], 2016, 109: 13
- Richer P, Yandouzi M, Beauvais L et al. *Surface and Coating Technology*[J], 2010, 204: 3962
- Cai J, Guan Q F, Hou X L et al. *Apply Surface Science*[J], 2014, 317: 360
- Zhang B Y, Meng G H, Yang G J et al. *Apply Surface Science*[J], 2017, 397:125
- Schumann E, Sarioglu C, Blachere J R et al. *Oxidation of Metals*[J], 2000, 53: 259
- Mumm D R, Evans A G, Spitsberg I T. *Acta Materialia*[J], 2001, 49: 2329
- Schlichting K W, Vaidyanathan K, Sohn Y H et al. *Materials Science and Engineering A*[J], 2000, 291: 68
- Zhang B Y, Yang G J, Li C X et al. *Apply Surface Science*[J], 2017, 406: 99
- Tomimatsu T, Zhu S, Kagawa Y. *Acta Materialia*[J], 2003, 51: 2397
- Xu R, Fan X L, Wang T J. *Apply Surface Science*[J], 2016, 370: 394
- Jiang J, Zhao H Y, Zhou X M et al. *Journal of Thermal Spray Technology*[J], 2013, 22: 69
- Wu B C, Chao C H, Chang E et al. *Materials Science and Engineering A*[J], 1990, 124: 215
- Lee D B, Ko J H, Yi Y H. *Journal of Thermal Spray Technology*[J], 2005, 14: 315
- Giovanni Pulci, Jacopo Tirillò, Francesco Marra et al. *Metallurgical and Materials Transactions A*[J], 2014, 45: 1401
- Mineaki Matsumoto, Takeharu Kato, Kazuyuki Hayakawa et al. *Surface and Coating Technology*[J], 2008, 202: 2743
- Li Y J, Xie Y T, Huang L P et al. *Ceramics International*[J], 2012, 38: 5113
- Wang P, He Y D, Zhang J. *Surface and Coating Technology*[J], 2015, 283: 37
- Ma X X, He Y D, Wang D R. *Apply Surface Science*[J], 2011, 257: 10273
- Deng S J, Wang P, He Y D et al. *International Journal of Minerals, Metallurgy and Materials*[J], 2016, 23: 704
- Yerokhin A L, Nie X, Leyland A et al. *Surface and Coating Technology*[J], 1999, 122: 73
- Gupta P, Tenhundfeld G, Daigle E O et al. *Surface and Coating Technology*[J], 2007, 201: 8746
- Nie X, Meletis E I, Jiang J C et al. *Surface and Coating Technology*[J], 2002, 149: 245
- Smith A, Kelton R, Meletis E I. *Plasma Chemistry and Plasma Processing*[J], 2015, 35: 963
- Deng S J, Wang P, He Y D. *Surface and Coating Technology*[J], 2015, 279: 92
- Anstis G R, Chantikul P, Lawn B R et al. *Journal of the American Ceramic Society*[J], 1981, 64: 533
- Evans H E. *Materials Science and Engineering A*[J], 1989, 120: 139

阴极等离子体电沉积 Pt 颗粒弥散的 Al₂O₃/YSZ 复合涂层的性能研究

邓舜杰¹, 蒋 驰², 刘天伟², 帅茂兵¹, 王 鹏³

(1. 表面物理与化学重点实验室, 四川 绵阳 621907)

(2. 中国工程物理研究院, 四川 绵阳 621900)

(3. 航天材料及工艺研究所, 北京 100076)

摘要: 采用阴极等离子体电沉积弥散 Pt 颗粒增韧 YSZ-Pt/Al₂O₃-Pt 双层复合涂层。涂层中弥散的 Pt 颗粒阻碍的氧在涂层中的扩散, 提高了涂层的抗氧化性能。Pt 颗粒的弥散增韧显著提高了涂层的断裂韧性, 缓解了陶瓷层与合金基体在高温下产生的热应力, 使得涂层在高温服役过程中具有良好的抗剥落性能。

关键词: 阴极等离子体电沉积; 抗高温氧化性能; 复合涂层; 颗粒增韧

作者简介: 邓舜杰, 男, 1988 年生, 博士, 助理研究员, 表面物理与化学重点实验室, 四川 绵阳 621907, 电话: 028-65726369, E-mail: shunjdeng@yahoo.com, 13708113923@163.com